Landmarks in Earth Reinforcement, Ochiai et al. (eds),
© 2001 Swets & Zeitlinger, ISBN 90 2651 863 3

Shaking table and numerical modelling of reinforced soil walls

M.M. El-Emam, R.J. Bathurst & K. Hatami
Geotechnical Research Group, Civil Engineering Department, Royal Military College of Canada, Kingston, Ontario, Canada

M.M. Mashhour
Professor and Head, Structural Engineering Department, Faculty of Engineering, Zagazig University, Zagazig, Egypt

ABSTRACT: The behaviour of reinforced soil walls under seismic loading is investigated using physical shaking table tests and numerical simulation, with particular emphasis on wall footing toe restraint conditions. A specially instrumented toe was designed to study the influence of toe restraint condition on model wall behaviour under static and dynamic loading. The model walls were instrumented to measure lateral facing displacement, reinforcement loads, load transmitted to the facing panel toe, and acceleration response along the height of the wall face and within the backfill. After construction, the models were subjected to a stepped amplitude sinusoidal base acceleration. Results from the experimental program were used to verify the accuracy of numerical models simulating seismic response of the shaking table tests using a finite difference-based computer program. The predicted responses from numerical models were found to be in general agreement with measured results. Both numerical and physical test results indicated that the toe restraint condition has a significant effect on the seismic response of the model walls. Some implications of the experimental and numerical modelling results to analysis and performance of propped-panel reinforced soil retaining walls are summarised.

1 INTRODUCTION

Seismic design methodologies that are currently used in North America for geosynthetic reinforced soil walls have been based largely on the results of numerical modelling of reinforced soil structures constructed with relatively in-extensible steel reinforcement (Bathurst and Alfaro 1996). Methods based on experience with in-extensible reinforcement are not necessarily applicable to walls using relatively extensible geosynthetic reinforcement products with respect to the required number/strength, location and length of reinforcement layers (Bathurst and Hatami 1998). A research strategy to update current approaches for seismic design of geosynthetic reinforced soil walls is to use numerical models that are validated against the results of carefully conducted shaking table tests on reduced-scale models of reinforced soil walls.

This paper presents selected results from a series of reduced-scale reinforced soil retaining wall models that were tested on a shaking table. The model walls were constructed with different toe boundary conditions and loaded to failure using a stepped-amplitude harmonic excitation record. Following the experimental tests, a calibrated numerical model was developed using a finite difference-based computer program to simulate the measured response of reduced-scale wall models to the shaking table base excitations.

2 MODEL SHAKING TABLE TESTS

2.1 *RMC shaking table*

The Royal Military College shaking table is comprised of a 3 m by 3 m steel platform driven by a 100 kN hydraulic actuator with a ±75 mm stroke range. The maximum payload capacity of the table is 4500 kgf. The table is capable of shaking a full payload at frequencies up to 13 Hz and peak base acceleration amplitudes up to 2g. A data acquisition/control system is used to drive the table using a prescribed displacement function. Test models are confined within a rectangular box 1.4 m wide by 3 m long that is bolted to the steel shaking table.

2.2 *Model configurations*

A series of fourteen 1 m-high models at 1/6 scale comprise the experimental portion of the research program. In order to predict the behaviour of equivalent (prototype) models at full scale, the model walls were designed in accordance with simulation rules proposed by Iai (1989). The reinforcement vertical spacing for the two models discussed in this paper was S_v = 0.23 m. The reinforcement length, L, was

chosen to give L/H = 0.6, where H is the height of the model (Figure 1).

In order to examine the influence of the toe restraint condition on model response, two different toe arrangements were used. The facing toe in different wall models was either hinged (restrained in the vertical and horizontal directions, while free to rotate) or sliding (restrained in the vertical direction only and free to rotate and slide horizontally).

2.3 *Materials*

The backfill soil used in all tests was a commercially available, manufactured clean uniformly graded sand. The primary reason for using this sand was to ensure a repeatable sand placement condition for all tests. The sand has a unit weight of 15.7 kN/m^3, peak direct shear friction angle of 52° and dilation angle of 14.5° when placed in a dense condition. At large strain and in a loose condition, the sand has a unit weight of 12.9 kN/m^3 and residual direct shear friction angle of 46°.

A knitted geogrid polyester product with a polyvinyl chloride coating and an aperture size of 45 mm by 25 mm was used as the reinforcement. The tensile strength of the geogrid was 1.8 kN/m at 2% strain and 3.25 kN/m at 5% strain in the loading direction. This particular geogrid was chosen because its stiffness in reduced-scale models falls in the range of typical reinforcement stiffness values at prototype scale.

The facing panel was constructed using rectangular hollow steel sections with cross-section dimensions 75 mm by 38 mm. A total of 26 sections were bolted together to form a 1 m-high rigid facing with a thickness of 75 mm and length of 1.4 m.

2.4 *Instrumentation*

Up to 64 instruments were installed in each test wall to monitor the following performance features of the models during construction and dynamic loading: (a) facing horizontal movements; (b) reinforcement displacements and strains; (c) horizontal and vertical toe loads; and, (d) facing and backfill acceleration response at different elevations.

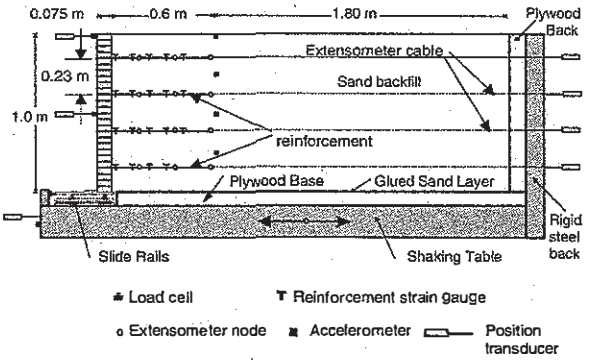

Figure 1. Test configuration and instrumentation for model walls.

A typical instrumentation layout and test wall configuration is shown in Figure 1. Cable-extension position transducers (extensometers) were used to measure facing displacements during base shaking. The body of each transducer was attached to a rigid vertical post mounted on the shaking table. This allowed the devices to record the relative movement of the model facing with respect to the table.

Local strain in the reinforcement was measured using strain gauges bonded to the polyester bundles of the longitudinal members. Extensometers were used to measure global strains, which are defined as strains measured over several geogrid apertures. Global strain measurements were used to confirm strain gauge readings and to convert strain values to load.

Acceleration response during shaking was measured using seven accelerometers, one of which was attached to the table to record the input base acceleration. Two accelerometers were attached to the facing and four were buried at different locations in the backfill as shown in Figure 1.

The forces transmitted from the facing panel to the footing (facing toe) were measured using vertical and horizontal load cells. The toe force was decoupled into horizontal and vertical components by using three linear roller bearings at the base. These roller bearings were used to reduce the friction in the horizontal direction at the toe and to ensure that the entire horizontal component of the toe force was transferred only to the horizontal load cells.

Two data acquisition systems were used to take data from 64 instruments at a sampling rate of 150 readings per second per channel. A high sampling rate was required to avoid aliasing effects and to capture the peak values of dynamic wall response induced by base shaking.

2.5 *Base excitation*

A stepped-amplitude, sinusoidal function with a frequency of 5 Hz was used to shake the models. The actuator stroke was increased at 5 second intervals to generate an equivalent incremental base acceleration of 0.05g until excessive model deformation occurred. The same base excitation history was applied to each model in order to allow quantitative comparisons to be made between different test configurations.

2.6 *Test results*

Due to space constraints, only selected test results are presented here. Typical displacements at the top of the wall facing versus input base acceleration for nominally identical model walls with L/H = 0.6 but with hinged and sliding toe boundaries are shown in

Figure 2. For the hinged toe model, the facing displacement was primarily a result of facing rotation. However, for the model wall with a sliding toe, the horizontal facing displacement was a combination of facing panel rotation and translation at the facing toe. For these reasons, the model wall with a sliding toe showed greater facing horizontal displacement at the top than the hinged toe model (Figure 2). It is clear from the figure that, the toe restraint condition affects the horizontal displacement significantly at input base acceleration magnitudes greater than 0.3g. At this acceleration level, the base of the sliding toe model started to slide outward dramatically.

The variation of the total vertical toe load with input base acceleration magnitude is shown in Figure 3. At the static condition (end of construction), the vertical toe load is about 75% greater than the weight of the facing column. This is due to down-drag forces acting on the back of the facing. Down-drag forces are the result of frictional shear forces developed between the soil and the facing column as well as the vertical component of forces at the connections due to settlement of the soil behind the facing. Down-drag forces increase with acceleration amplitude of base shaking. However, the toe condition does not have significant effect on the magnitude of vertical load developed at the toe.

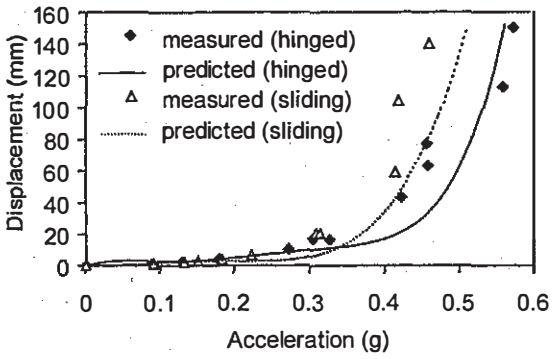

Figure 2. Measured and predicted displacement at the top of the model facing vs. base acceleration amplitude.

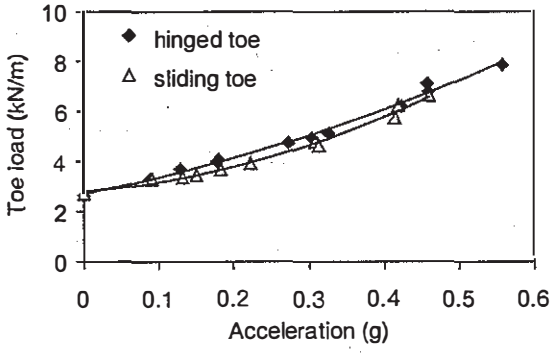

Figure 3. Vertical toe load for models with sliding and hinged toe boundary conditions vs. input base acceleration.

Figure 4 shows the magnitude and distribution of the peak load (static condition and during base excitation) in the reinforcement layers at the wall connections for nominally identical sliding and hinged toe models. The plots for the hinged toe model also include horizontal toe loads. The load distributions are plotted for different input base acceleration magnitudes. The data show that reinforcement connection loads and toe loads increase with magnitude of input acceleration amplitude. The top reinforcement layer did not develop any additional load during shaking. This may be attributed to the small overburden pressure on the top layer (0.15 m from the top of the model) which resulted in slippage of the reinforcement layer in the soil. The reinforcement connection load in the bottom layer increased significantly under severe shaking in the final stages of both test configurations. For base input acceleration values greater than 0.1g, the reinforcement connection loads at the second and third layer below the top of the wall are greater for the hinged toe model than for the sliding toe model. This result demonstrates that the toe boundary condition will influence not only the magnitude of reinforcement loads but also the distribution of loads under large base accelerations.

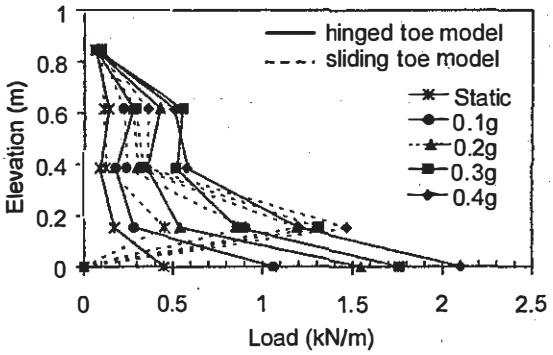

Figure 4. Measured connection and toe loads for models with sliding and hinged toe boundary vs. elevation at different input base accelerations.

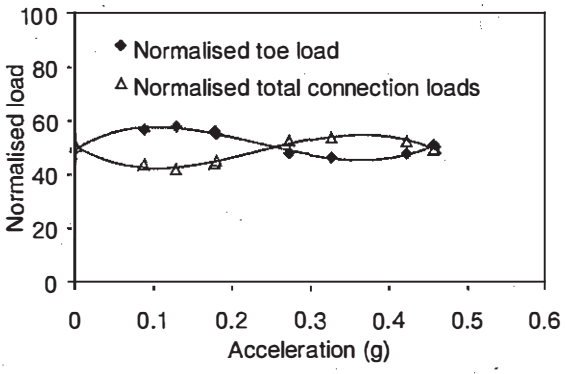

Figure 5. Toe load and sum of connection loads normalised to the total earth force for model with hinged toe vs. input base acceleration amplitude.

Figure 5 illustrates that at the end of construction, the horizontal toe load (in these experiments) is equal to the sum of connection loads. This observation is consistent with full-scale instrumented wall tests that have shown that a restrained footing may contribute significant earth pressure capacity to geosynthetic reinforced walls constructed with a structural facing under static loading (Bathurst and Walters 2000). As the acceleration amplitude increased, a slightly larger portion of the total earth force behind the facing panel was taken by the toe. When the input base acceleration exceeded 0.3g, the reinforcement started to attract more load than the toe. An explanation for this behaviour is that at a base acceleration amplitude of 0.3g, soil-reinforcement interaction is fully mobilised and the reinforcement layers begin to take a larger portion of the load. Nevertheless, over the entire course of the test the toe and reinforcement layers each attracted roughly 50% of the total static and dynamic earth pressure.

Outward (away from the soil) acceleration amplification factors plotted against input base acceleration amplitude are shown in Figure 6. It is clear from the figure that prior to an acceleration amplitude of 0.3g, all outward acceleration amplification factors are small but increase significantly thereafter. A possible explanation is that soil dilation during shaking leads to a reduction in stiffness of the system and a corresponding larger amplification factor. Increasing magnitude of amplification factor with increasing base excitation for extensible reinforcement shaking table models has also been reported by Matsuo et al. (1998). These results are in contrast to results of studies using relatively in-extensible metallic reinforced soil wall models that showed that acceleration amplification magnitude decreases with base acceleration amplitude (e.g. Richardson and Lee 1975, Fairless 1989). In general, the outward acceleration amplification factors are larger for the model with a hinged toe than for the model with a sliding toe. This observation is in accordance with numerical results for prototype-scale propped panel walls subjected to base excitation reported by Bathurst and Hatami (1998). Figure 6 also shows that there is a phase difference between input base acceleration and response accelerations for both hinged and sliding toe model walls. Out-of-phase motions in the soil can be expected to have a marked effect on the distribution of dynamic reinforcement load with time during base excitation (e.g. Steedman and Zeng 1990).

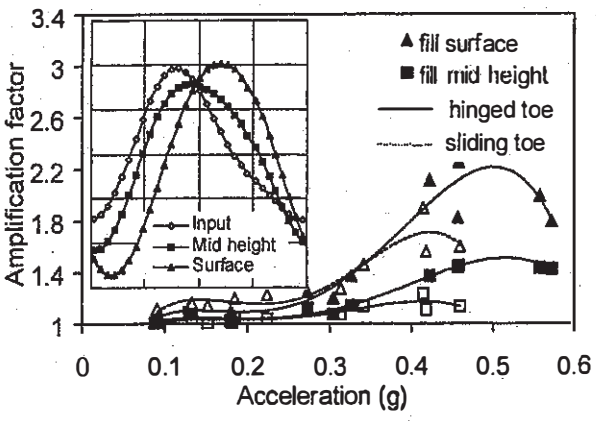

Figure 6. Amplification factors for hinged and sliding base models vs. input base acceleration.

3 NUMERICAL SIMULATION

3.1 *Numerical model and material properties*

The results obtained in the experimental part of this research were used to develop a calibrated numerical model using the finite difference-based, two-dimensional stress analysis program FLAC (Itasca 1998). Figure 7 shows the details of a typical numerical configuration that was used in the analyses. The soil was modelled using an elastic-plastic strain softening model with Mohr-Coulomb failure criteria. Material parameters used to model soil were: peak friction angle, ϕ_p ; cohesion, c ; residual friction angle, ϕ_{cv} ; dilation angle, ψ ; shear modulus, G; and bulk modulus, K. The numerical values for soil parameters were established by calibrating a numerical model to give the same load-deformation response as physical direct shear tests. Direct shear tests were carried out on the same sand prepared to the same density as the shaking table models. The geosynthetic reinforcement was modelled using linear elastic perfectly plastic, two-noded cable elements with axial stiffness, J = 78 kN/m. The cable elements had negligible bending stiffness and compressive strength. The stiffness of the geogrid was determined from load-elongation curves produced from wide-width strip tensile tests.

The base input motion was introduced to the wall models by applying a prescribed horizontal velocity and zero vertical velocity to the nodes at the base

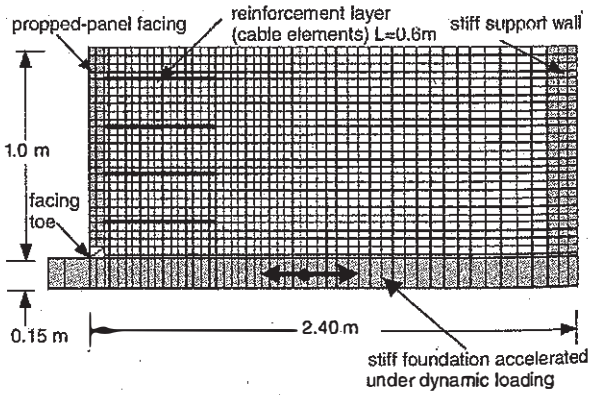

Figure 7. Numerical grid for the reinforced soil model wall with fixed toe condition.

of the numerical grid. The applied velocity was increased in a stepwise manner to match the experimental input acceleration history until excessive deformation occurred.

3.2 *Comparison of numerical and physical results*

Calculated and measured maximum displacement values versus input acceleration for the hinged and sliding model walls described earlier are shown in Figure 2. It should be noted that the hinged-toe and sliding-toe models became unstable at base acceleration amplitudes equal to 0.4g and 0.35g, respectively. In addition, it can be seen that the predicted and measured facing displacements show good agreement. The figure shows that the sliding toe model wall recorded larger top displacements than the hinged toe model wall in both physical tests and numerical simulations.

A comparison of the vertical and horizontal toe loads calculated using numerical analysis and measured in the physical tests is shown in Figure 8. The numerical model results are in reasonable agreement with the experimental data. It can be seen that the numerical simulation captured the trend of slightly lower magnitude of vertical toe load measured for the sliding toe model compared to the hinged toe

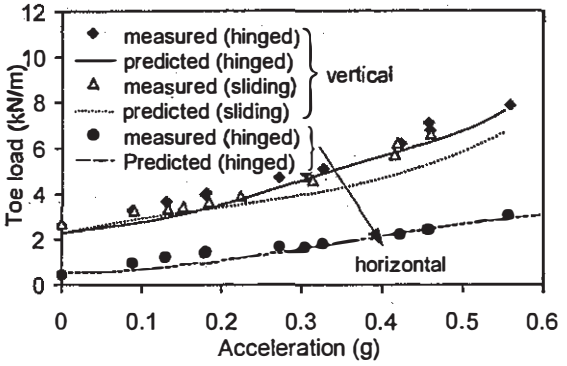

Figure 8. Measured and predicted toe loads for model walls vs. input base acceleration.

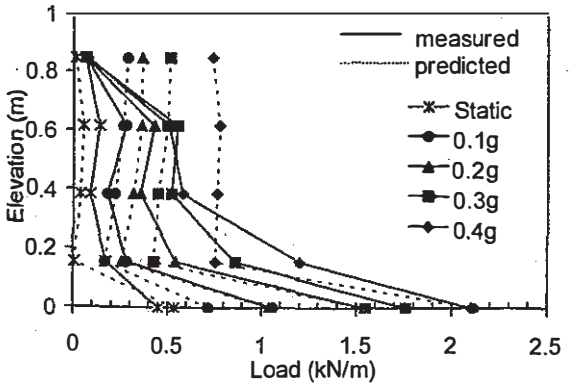

Figure 9. Measured and predicted connection and toe loads at different input base acceleration for hinged toe model.

model (see also Figure 3). This observation may be attributed to a larger amount of soil mass that passed outward beyond the heel of the wall face as a result of the slightly larger rotation of the facing panel for the hinged toe model.

The accuracy of predicted connection loads in Figure 9 is reasonably good over the middle of the wall height (up to 0.3g) and at the toe. The predicted top layer response is poor. This is likely the result of reinforcement slip which was not modelled in numerical simulations (i.e. the reinforcement layers were taken as fully bonded to the sand soil). This observation highlights the requirement to include interface slip in numerical models for reinforcement layers under low overburden pressures. However, the numerical results do demonstrate that the facing toe attracted a significant portion of the total horizontal earth pressure at all stages of the simulation and therefore reduced the demand on the reinforcement layers.

4 CONCLUSIONS AND IMPLICATIONS TO DESIGN

Selected results of shaking table tests on reduced-scale, reinforced soil retaining walls with $L/H = 0.6$ and a vertical spacing $S_v = 0.23$ m are reported together with numerical modelling. The investigation is focused on the influence of the toe boundary condition on lateral displacements, reinforcement loads, toe loads and acceleration amplification in the backfill. The following conclusions can be made:

1. The displacement response for the model wall with a sliding toe was greater than the response of the model with a hinged toe when base acceleration amplitude exceeded 0.3g.

2. The vertical toe load was found to be greater than the facing self-weight throughout each experiment, due to downdrag forces, and increased as the input base acceleration increased.

3. The type of toe boundary condition did not influence the magnitude of vertical toe loads generated at end of construction (static) and under dynamic loading.

4. The footing for models with a restrained toe attracted approximately 50% of the static and dynamic horizontal earth force acting against the back of the facing panel. The magnitude and distribution of reinforcement loads was observed to be influenced by the boundary toe condition. In particular, reinforcement load in the bottom reinforcement layer was greater for the unrestrained toe case compared to the hinged toe case.

5. Input base acceleration was amplified towards the backfill surface. The amplification factor was found to be about 1.2 for input accelerations lower

than 0.3g, and increased sharply to about 2.2 for greater input base acceleration amplitudes. The trend of increasing amplification factor with increasing base acceleration is reversed from the trend reported in the literature for reduced-scale reinforced soil walls constructed with relatively in-extensible reinforcement layers.

6. Overall, the numerical response results of model walls subjected to base excitation were found to be in close agreement with the measured data with the exception of predicted reinforcement loads for reinforcement layers under low overburden depths.

The results of this investigation have important implications to the design of geosynthetic reinforced soil retaining walls under static loading and in seismic environments. The contribution of a restrained toe to wall load capacity and the distribution of reinforcement loads is not considered in current pseudo-static design methods. Neglecting the load-carrying capacity of a laterally restrained facing toe may result in over estimation of reinforcement design loads and unsafe design of the footing. Downdrag forces acting against the back of a rigid facing column can be expected to place additional loads on the connections and the footing. These additional loads are not considered in current North American practice and hence current practice may be unsafe in this regard. The acceleration amplification and phase lag along the wall height and in the backfill observed in the physical tests are not considered in current pseudo-static design methods for reinforced soil retaining walls. The trend of increasing acceleration amplification with increasing base acceleration observed for the walls in this study is opposite to that reported in the literature for metallic reinforced soil wall experiments. Hence, empirical design rules based on reinforced soil walls with metallic reinforcement materials may not apply to walls constructed with relatively extensible reinforcement products.

REFERENCES

Bathurst R.J. & M.C. Alfaro 1996. Review of seismic design analysis and performance of geosynthetic reinforced walls, slopes and embankments. Earth Reinforcement, Ochiai H., N. Yasufuku & K. Omine (eds), Balkema: 2, *Proc. of Intern. Symp. on Earth Reinf. Fukuoka, Kyushu, Japan, November 1996 Keynote Lecture:* 887-918.

Bathurst, R.J. & D.L. Walters 2000. Lessons learned from full scale testing of geosynthetic reinforced soil retaining walls, *GeoEng2000*, Melbourne, Australia, November 2000, 14 p.

Bathurst R.J. & K. Hatami 1998. Seismic response analysis of a geosynthetic-reinforced soil retaining Wall. *Geosyn. Intern. 5(1-2):* 127-166.

Fairless, G.J. 1989. Seismic performance of reinforced earth walls. *Research report 89-8, Dept. Civ. Eng., Univ. of Canterbury*, Christchurch, New Zealand.

Iai S. 1989. Similitude for shaking table tests on soil-structure-fluid models in 1g gravitational field. *Soils Found. 29(1):* 105-118.

Itasca 1998. *Fast Lagrangian analysis of continua ver. 3.4.* Itasca Consult. Group Inc. Minneapolis, MN, USA.

Matsuo O., T. Tsutsumi, K. Yokoyama & Y. Saito 1998. Shaking table tests and analyses of geosynthetic-reinforced soil retaining walls. *Geosyn. Intern. 5(1-2):* 97-126.

Richardson G.N. & K. Lee 1975. Seismic design of reinforced earth walls. *ASCE, Proc. J. Geotech. Eng. Div. 101(GT2):* 167-187.

Steedman R.S. & X. Zeng 1990. The influence of phase on the calculation of pseudo static earth pressure on retaining walls. *Geotechnique. 40(1):* 101-112.